IBRO Neuroscience Reports 15 (2023) 376–385

Contents lists available at ScienceDirect

IBRO Neuroscience Reports

journal homepage: www.sciencedirect.com/journal/IBRO-Neuroscience-Reports

A key protein from *Borrelia burgdorferi* could stimulate cytokines in human microglial cells and inhibitory effects of Cucurbitacin IIa

Xin Xu [a,c,d], Shiyuan Wen [a,c,e], Yu Zhang [a,c,d], Wenjing Cao [a,b], Peng Yue [a,b], Jing Kong [a,c], Meixiao Liu [a,c], Yuxin Fan [a,c], Jingjing Chen [a,c], Zhenhua Ji [a,c], Yan Dong [a,c], Guozhong Zhou [a,c], Bingxue Li [a,c], Aihua Liu [a,c,d,*], Fukai Bao [a,c,d,*]

[a] The Institute for Tropical Medicine, Faculty of Basic Medical Sciences, Kunming Medical University, Kunming, China
[b] Department of Biochemistry and Molecular Biology, Kunming Medical University, Kunming, China
[c] Department of Microbiology and Immunology, Kunming Medical University, Kunming, China
[d] Yunnan Province Key Laboratory of Children's Major Diseases Research, The Affiliated Children Hospital, Kunming Medical University, Kunming, China
[e] Department of Intensive Care Unit, First People's Hospital of Yunnan Province, Kunming, China

ARTICLE INFO

Keywords:
Cucurbitacin IIa
Cytokine
Inflammation
Lyme neuroborreliosis
Microglia
RBmpA

ABSTRACT

Lyme neuroborreliosis (LNB) is an infectious disease of the nervous system caused by *Borrelia burgdorferi (Bb)* infection. However, its pathogenesis is not fully understood. We used recombinant BmpA (rBmpA) to stimulate human microglia cell HMC3, then collected the culture supernatant and extracted total RNA from cells, and used the supernatant for cytokine chip, then ELISA and qPCR technology were used to validate the results from cytokine chip. After rBmpA stimulation of microglia, 24 inflammation-related cytokines showed elevated expression. Among them, six cytokines (IL-6, IL-8, CCL2, CCL5, CXCL1, and CXCL10) increased significantly in mRNA transcription, three cytokines (IL-6, IL-8, and CXCL10) concentrations in the cell supernatant increased significantly after the rBmpA stimulation, and CuIIa could inhibit expression of these cytokines. The BmpA can stimulate human microglia to produce large amounts of cytokines, leading to the occurrence of inflammation, which may be closely related to the development of LNB. CuIIa can inhibit BmpA-induced cytokine production in microglia, which may have potential therapeutic effects on LNB.

1. Introduction

Lyme neuroborreliosis (LNB) is an infectious disease of the nervous system caused by *Borrelia burgdorferi (Bb)* infection (Koedel et al., 2015). *Bb* is highly neurophilic and can remain latent in the central or peripheral nervous system for long periods of time, inducing different neuropathies at different stages, with neurological involvement in up to 20% of Lyme disease patients (Koedel and Pfister, 2017). LNB of the central nervous system (CNS) mostly manifests as meningitis, and LNB of the peripheral nervous system (PNS) mostly manifests as sensory abnormalities, hemiparesis, and spasticity (Halperin, 2014). Common effects of LNB include lymphocytic meningitis, cranial neuritis, and painful radiculitis, others such as myelitis, peripheral neuritis, and cerebellar ataxia can also occur (Marques, 2015). LNB is characterized by recurrent and progressive exacerbations, and some patients may develop memory loss, dementia, and personality disorders (Pachner and Steiner, 2007). Therefore, it is important to further investigate the pathogenesis of LNB.

Borrelia burgdorferi basic membrane protein A (BmpA) is a major virulence factor that is closely associated with Lyme arthritis (Pal et al., 2008). Expression of the gene encoding BmpA, *bmpA*, is clearly elevated in mouse joints relative to skin, heart, and bladder tissues. A *bmpA* knock-out *B. burgdorferi*-strain failed to induce arthritis, while knock-in of the *bmpA* gene recovered the ability of spirochetes to induce this condition (Pal et al., 2008). Our previous studies have reported that recombinant BmpA (rBmpA) can cause pro-inflammatory responses in human synovial cells, THP-1 macrophages, THP-1 dendritic cells, and RAW264.7 cells, and that, by inducing the expression of TNF-α, IL-1β, and IL-6, intra-joint injection of rBmpA leads to Lyme arthritis in a mouse model (Yang et al., 2008, Zhao et al., 2017b; 2017a). Moreover, murine microglia stimulated with rBmpA produce specific chemokines, which may influence the development of LNB (Zhao et al., 2017b;

* Corresponding authors at: The Institute for Tropical Medicine, Faculty of Basic Medical Sciences, Kunming Medical University, Kunming, China.
E-mail addresses: liuaihua@kmmu.edu.cn (A. Liu), baofukai@kmmu.edu.cn (F. Bao).

https://doi.org/10.1016/j.ibneur.2023.11.004
Received 1 April 2023; Accepted 9 November 2023
Available online 13 November 2023

2017a). Based on these studies, we intended to further consolidate the correlation between rBmpA and the pathogenesis of LNB.

Microglia, a type of glial cell, account for one-tenth of the total number of cells in the adult nervous system and are the resident phagocytic cells of the CNS, constituting the brain's first line of immune defense and are known as "macrophages" of the CNS (Dello Russo et al., 2018). It has been shown that in animal models of Lyme disease, CNS invasion leads to local tissue damage as a result of potent induction of pro-inflammatory mediators by microglia (Pachner et al., 2002, Isogai et al., 1996). Microglia are resident immune cells within the CNS and derive from circulating monocytes with a slow conversion rate (Colonna and Butovsky, 2017). When activated, microglia are able to mount a strong and rapid immune response to invading pathogens and coordinate infiltration of peripheral blood leukocytes (Aloisi, 2001). Our previous study found that the concentrations of CXCL2, CCL22, and CCL5 chemokines in mouse microglia BV2 cells increased with increasing concentrations of BmpA, and the mRNA expression levels of these chemokines in the cells also significantly increased (Zhao et al., 2017b; 2017a). Therefore, we reasoned that the chemokines in LNB may be mainly produced by microglia.

There are 31 species of the *Hemsleya* plant. With the exception of two species, which grow in India and Vietnam, 29 species are distributed across the Yunnan, Guizhou, and Sichuan provinces of China (Peng et al., 2020). In recent years, with the development and maturity of phytochemistry and natural product chemistry, researchers have extracted and isolated two major natural products from the tuber of *Hemsleya macrosperma*, Cucurbitacin IIa (CuIIa) and Cucurbitacin IIb (CuIIb) (Recio et al., 2004, Wang et al., 2017). CuIIa, a tetracyclic triterpenoid compound, is the major bioactive component of *H. macrosperma* and has been attracting much attention for its antiviral and anti-inflammatory properties (Zeng et al., 2021). Although many studies have described the pharmacological activities of CuIIa, the effects of CuIIa on inflammation of LNB have not been investigated (Zeng et al., 2021; 2017, Boykin et al., 2011). Therefore, in the present study, we examined the anti-inflammatory effect of CuIIa against BmpA-induced inflammation.

2. Materials and methods

2.1. HMC3 cell culture

The human microglial clone 3-cell line, HMC3, was established in 1995, through SV40-dependent immortalization of human embryonic microglial cells (Dello Russo et al., 2018). Since the HMC3 cell line retains most of the morphological, phenotypical, and functional properties described for freshly isolated microglial cells, it has been used extensively as one of the most common microglial cells in neurodegenerative disorders research (Angel-Ambrocio et al., 2020, Hankittichai et al., 2020). HMC3 cells (Shanghai ZhongQiao XinZhou Biotechnology Co, Shanghai, China) were cultured in Minimum Essential Medium (MEM; Gibco) with 10% fetal bovine serum (FBS; Gibco) and 1% penicillin/streptomycin (Thermo Fisher) at 37 °C and 5% CO_2. The cells were seeded in a 6-well plate (Corning, USA) at 2.5×10^5 cells/mL and cultivated for 12 h until they were fully adherent to the plate.

2.2. Cytotoxicity assay of CuIIa

The pure CuIIa (98.00%) was kindly provided by Yunnan Yizhihao Co., Ltd. (China), and the purity of CuIIa was assayed by high performance liquid chromatography (HPLC; Chengdu Must Bio-Technology Co., Ltd). The chemical structure of CuIIa is 23, 24-dihydrocucurbitacin F-25-acetate, so it is called Cucurbitacin IIa (CuIIa), and its molecular formula is C32H50O8. First, we prepared 0.2 mol/L of CuIIa. The pure solid CuIIa, a tetracyclic triterpenoid compound with a molecular weight of 562.7 g/mol, was dissolved in dimethyl sulfoxide (DMSO). Weigh 0.9 g CuIIa and dissolve in 8 mL DMSO, that is, prepare 0.2 mol/L CuIIa. Then dilute it according to the concentration required by the experiment. Cell Counting Kit (CCK-8) (Dalian Meilun Biotechnology Co., Ltd., Dalian, China) was used to detect cytotoxic concentrations of CuIIa. The HMC3 cells were plated at a density of 1.3×10^4 cells per well in a 96-well plate (Eppendorf, Germany) and incubated overnight. Cells were then treated with different concentrations of CuIIa (1, 12.5, 25, 50, 100, and 200 μM). After incubation at 37 °C for 24, 48, and 72 h time points, medium containing 10% CCK-8 solution was added to each well and incubated for 2.5 h. A BioRad microplate reader (Model 680, BioRad Laboratories, Inc., Hercules, CA, USA) was used to measure the absorbance at 450 nm. The cell viability in chemically treated groups was defined as the percentage of control cells.

2.3. Recombinant BmpA preparation

Recombinant BmpA (rBmpA) was produced in *Escherichia coli* (*E.coli*) using the bacterial expression vector pGEX-6P1 (GE, USA) and the following primers (5′−3′ containing *EcoR*I and *Xho*I restriction sites): ACG AAT TCA TGA ATA AAA TAT TGT TGT TGA, AGC TCG TAA ATA AAT TCT TTA AGA AA (Pal et al., 2008). Expression, purification, and enzymatic cleavage of the glutathione S-transferase (GST) fusion protein was carried out as previously described (Yang et al., 2008, Zhao et al., 2017b; 2017a). In order to eliminate the possibility that rBmpA were contaminated with *E.coli*-derived LPS, the purified rBmpA samples were tested by the limulus test. If rBmpA contaminated, polymyxin B was added to the sample to neutralize LPS contamination (Cooper et al., 1972, Cardoso et al., 2007, Tsuzuki et al., 2001).

2.4. Stimulation and sample collection

Many studies have shown that Cucurbitacin has significant anti-inflammatory activity (Zeng et al., 2021, Cai et al., 2015, Delgado-Tiburcio et al., 2022). Studies have found that Cucurbitacin can pass through cell membranes, and then it can up-regulate or down-regulate certain protein signaling molecules, activating signaling pathways, such as TLR-like signaling pathways, to play an anti-inflammatory role (Park et al., 2015, Varela et al., 2022). There have also been studies on the immune response of Cucurbitacin, which have been found to play a role in both innate and adaptive immunity. The most cited mechanisms are inhibition of COX-2 and NOS, reduction of oxidative stress, inhibition of pro-inflammatory cytokines, and regulation of acquired immune proteins (Silvestre et al., 2022). Therefore, Cucurbitacin mainly achieves anti-inflammatory effect by regulating inflammatory response, rather than directly interacting with rBmpA to play its function. Cells were cultured in an incubator (37 ℃, 5% CO_2) until they fully adhered to the 6-well plate, which took about 12–14 h, and then the supernatant were discarded. Cells were divided into four groups (negative control group, LPS-positive control group, and two experimental groups) and were stimulated, respectively, with normal medium, 1.2 ng/μL LPS, 40 μg/mL rBmpA, and 40 μg/mL rBmpA with 50 μM CuIIa. Culture supernatants were collected at 6, 12, 24, and 48 h after stimulation and were stored at − 80 ℃ for later use. After collecting the supernatants, 700 μL RNAiso plus (Takara, Japan) was added into every well to prepare cell lysates. Cells lysates were collected into RNAase-free tubes at different time points and stored at − 80 ℃ until RNA extraction.

2.5. Bio-Plex Pro™ human inflammation array assays

We collected 200 μL cell culture supernatant of each group at four time points (6, 12, 24, and 48 h). Those supernatant samples were detected by The Bio-Plex Pro™ human inflammation panel I (Bio-Rad, USA). The Bio-Plex Pro™ human inflammation panel I consists of a wide range of assays to facilitate the study of pro- and anti-inflammatory cytokines in various pathophysiological conditions. The assays are compatible with a wide variety of sample matrices, including serum,

plasma, and culture supernatant. For researchers working with limited sample volume, the capacity to multiplex will provide an effective option over the traditional ELISA method. The Bio-Plex Pro™ human inflammation panel I implements quantitative measurement of 48 human inflammatory cytokines, following the manufacturer's instructions.

2.6. Preparation of RNA and real-time quantitative polymerase chain reaction

After 6, 12, 24, and 48 h culture, the cell lysates were collected from each group for the extraction of total RNA. RNAiso Plus (Takara, Japan) was used to collect total RNA of cells. Then, RNA was extracted with chloroform-isopropanol. After incubation for 30 min, samples were centrifuged to isolate RNA and then washed with 75% ethanol. RNA concentration and purity were determined with a Nanodrop-2000 spectrophotometer (Thermo Fisher Scientific), and the approved samples [absorbance at 260 nm (OD260) $<$ 1.7 and OD280 $<$ 2.0] were stored at − 80 °C. The PrimeScript™ RT reagent kit with gDNA Eraser (Takara, Japan) was used to obtain cDNA. The reaction mixture contained the following: 1 μg RNA, 4 μL 5 ×PrimeScript Buffer 2 [for real-time quantitative polymerase chain reaction (qPCR)], 1 μL PrimeScript RT Enzyme Mix I, 1 μL RT Primer Mix, and RNase free dH2O in a final volume of 20 μL. The reaction was performed on a C1000 Touch thermal cycler (Bio-Rad, Hercules, CA, USA) under the following conditions: 37 °C for 15 min, 85 °C for 5 s, and 4 °C for an unlimited duration. The cDNA samples were stored at − 20 °C.

The qPCR was performed using SYBR Green Premix Ex Taq II (TliRNaseH Plus, 2 ×) (Takara, Japan) on a CFX96 Real-Time PCR system (Bio-Rad) according to the manufacturer's protocol. Four biological replicates were set for each group of samples, and two technical replicates were set for each biological replicate. The reaction volume was 25 μL, containing 12.5 μL of Takara SYBR Premix Ex Taq II (Tli RNaseH Plus, 2 ×), 1 μL of each primer, 2 μL of the cDNA template, and 8.5 μL RNase free dH2O. Amplification conditions were as follows: 95 °C for 30 s, followed by 40 cycles of 95 °C for 5 s, 60 °C (58.5 °C for *β-actin*) for 30 s. Relative gene expression levels were calculated with the comparative cycle threshold method with normalization to the housekeeping gene *β-actin*. The reliability of the experimental results was determined by the cycle threshold obtained from CFX96 Real-Time PCR system. When the cycle threshold of the target gene was 15–35 cycles and the cycle threshold of the reference gene was 15–25 cycles, the detection result of qPCR was credible. The sequences of specific primers used to amplify reference gene (*β-actin*), IL-6, IL-8, CCL2, CCL5, CXCL1, and CXCL10 are shown in Table 1. All primers were obtained from Tsingke Biotech (Beijing, China).

2.7. Enzyme-linked immunosorbent assay measurement

Based on the results of cytokine chip, several increased cytokines were estimated by Enzyme-linked immunosorbent assay (ELISA) to confirm the results from the chip. Culture supernatants were analyzed by ELISA for IL-6, IL-8 and CXCL10. ELISA was performed using Human IL-6 ELISA kit, Human IL-8 ELISA kit, and Human CXCL10 ELISA kit (Dakewe Bio-engineering Co., Ltd, Shenzhen, China) following the manufacturer's instructions. Three biological replicates were set for each group of samples. A Bio-Rad microplate reader (Model 680; Bio-Rad Laboratories, Inc., Hercules, CA, USA) was used to measure the absorbance at 450 nm.

Table 1
Gene primers in this study.

Gene	Forward primer (5' - 3')	Reverse primer (5' - 3')
il-6	ACTCACCTCTTCAGAACGAATTG	CCATCTTTGGAAGGTTCAGGTTG
il-8	ACTGAGAGTGATTGAGAGTGGAC	AACCCTCTGCACCCAGTTTTC
ccl2	GCAGCAAGTGTCCCAAAGAA	TCGGAGTTTGGGTTTGCTTG
ccl5	GAAAGAACCGCCAAGTGTGT	AAGAGCAAGCAGAAACAGGC
cxcl1	ACCGAAGTCATAGCCACACT	TCACTGTTCAGCATCTTTTCGA
cxcl10	GCCATTCTGATTTGCTGCCT	GCAGGTACAGCGTACAGTTC
β-actin	TGGCATCCACGAAACTACCT	CAATGCCAGGGTACATGGTG

2.8. Statistical analysis

Data were expressed as mean ± SEM and analyzed by two-way ANOVA using GraphPad Prism 8.0 (GraphPad, San Diego, CA, USA). Statistical significance was set at a P value of $<$ 0.05.

3. Results

3.1. Toxicity of the CuIIa to HMC3

We measured the cytotoxicity of CuIIa in HMC3 cells. HMC3 cells were treated with different doses of CuIIa (1, 12.5, 25, 50, 100, and 200 μM) for 24, 48, and 72 h, and cell viability was evaluated by CCK-8 assay. The cell relative growth rate was set as 100% in the negative control group (CuIIa, 0 μM). Four biological replicates were performed at each concentration. When CuIIa was 1 μM, the mean cell viability at 24, 48 and 72 h was 93.46%, 124.46% and 149.51%, respectively. When CuIIa was 12.5 μM, the mean cell viability at 24, 48 and 72 h was 69.91%, 68.85% and 64.95%, respectively. When CuIIa was 25 μM, the mean cell viability at 24, 48 and 72 h was 76.92%, 75.34% and 72.14%, respectively. When CuIIa was 50 μM, the mean cell viability at 24, 48 and 72 h was 74.79%, 73.17% and 80.24%, respectively. When CuIIa was 100 μM, the mean cell viability at 24, 48 and 72 h was 71.39%, 51.97% and 38.29%, respectively. When CuIIa was 200 μM, the mean cell viability at 24, 48 and 72 h was 44.38%, 40.39% and 15.62%, respectively. The result is shown in Fig. 1. From the result, we can see that different concentration of CuIIa have different toxicity in HMC3. We found that CuIIa at 1 μM promoted cell growth with increasing time compared to the negative control. However, when CuIIa concentrations reached 100 μM and 200 μM, cell viability was low and further decreased with time. The cell viability was higher when CuIIa concentrations were 12.5, 25, and 50 μM, and there was no statistical cell viability difference under these CuIIa concentrations at different time points, which met the experimental requirements. In addition, the highest mean cell viability was observed at 50 μM CuIIa, so we chose 50 μM CuIIa for the later experiments.

3.2. Cytokine chip results of HMC3 cell supernatant

Our cytokine liquid array detected a total of 48 cytokines associated with human inflammation, and the data is shown in Table 2. Twenty-four of these cytokines varied in different groups at different time points, and another 24 factors were not detected or their levels were

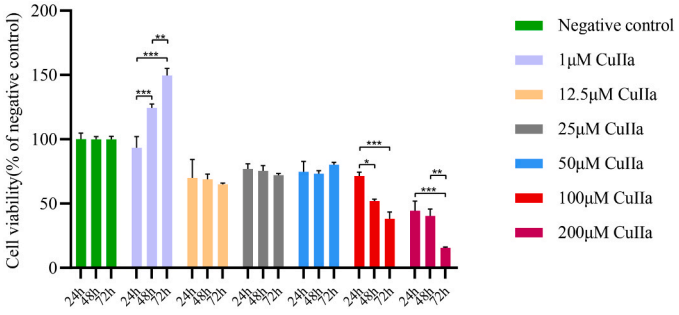

Fig. 1. Cell viability of HMC3 cells was detected by CCK-8 assay. Comparison of cell viability at different doses of CuIIa (1, 12.5, 25, 50, 100, and 200 μM). The two-way ANOVA and Tukey's multiple comparison test were used to evaluate the statistical significance between mean ± SEM of quadruplicate data sets. * $P < 0.05$, * * $P < 0.01$, * ** $P < 0.001$.

Table 2
Concentrations of 48 cytokines detected by cytokine liquid array (pg/mL).

Chemokine	6 h				12 h				24 h				48 h			
	PBS	LPS	rBmpA	rBmpA+CuIIa	PBS	LPS	rBmpA	rBmpA+CuIIa	PBS	LPS	rBmpA	rBmpA+CuIIa	PBS	LPS	rBmpA	rBmpA+CuIIa
CTACK/CCL27	3.82	15.64	14.62	8.11	5.05	21.32	16.96	8.32	7.5	29.74	23.55	9.95	12.19	36.75	29.23	11.98
Eotaxin/CCL11	1.74	13.64	7.41	1.78	2.91	29.53	14.94	1.39	7.28	38.37	21.99	2.23	13.48	46.14	22.48	1.32
basic FGF	2.25	9.12	8.25	4.57	3.14	11.11	8.25	3.9	6.31	17.88	12.56	9.54	10.73	24.11	17.88	21.89
G-CSF	21.26	210	86.89	61.68	33.78	297.19	147.43	110.84	94.19	829.53	318.82	279.31	209.38	1553.23	586.77	602.23
GM-CSF	0	5.08	3.15	0.35	0.18	8.63	4.23	0.18	0.93	25.6	5.25	1.54	3.19	74.92	12.76	2.44
Gro-α/CXCL1	**0**	**1526.35**	**1251.75**	**331.76**	**5.33**	**2177.89**	**1480.62**	**362.57**	**177.79**	**2714.62**	**1817.51**	**402.81**	**359.75**	**3479.68**	**2327.52**	**541.38**
HGF	0	11.96	6.19	4.23	0.19	17.66	13.87	2.24	6.19	43.68	21.42	15.77	15.77	63.81	38.15	27.03
IFN-α2	0	0	0	0	0	0.86	0	0	0	3.18	1.83	0	0.47	4.86	2.39	1.52
IFN-γ	0	5.97	2.75	0.69	0	8.78	5.05	0.17	2.24	13.66	7.22	2.49	3.5	19.06	10.21	4.22
IL-1α	0	0.42	0	0	0	1.62	0.92	0	0.26	6.84	3.06	1.62	1.97	10.74	5.31	4.93
IL-1β	0	0.05	0.05	0	0	0.4	0.19	0	0.05	0.9	0.42	0.19	0.29	1.44	0.77	0.58
IL-1Ra	0	0	0	0	0	0	0	0	0	0	0	0	0	27.12	0	0
IL-2	0	0	0	0	0	0	0	0	0	0	0	0	0	0.14	0	0
IL-2Ra	0	4.13	2.35	0.9	0.14	5.88	4.48	1.63	1.99	12.07	7.61	4.66	4.83	18.16	11.73	8.99
IL-3	0	0	0	0	0	0	0	0	0	0	0	0	0	0.19	0	0
IL-4	0	0.17	0.06	0	0	0.31	0.12	0.06	0.06	0.61	0.28	0.13	0.17	0.82	0.49	0.33
IL-5	4.99	59.64	59	42.85	15.91	78.13	70.19	26.39	40.24	96.43	88.88	48.69	59	108.98	108.36	62.21
IL-6	**746.31**	**3769.04**	**3572.22**	**1707.22**	**973.52**	**5589.91**	**4287.84**	**1448.38**	**1604.3**	**6966.42**	**6096.62**	**2521.63**	**3324.39**	**7405.62**	**7292.33**	**3003.71**
IL-7	0	0	0	0	0	0	0	0	0	0	0	0	0	0.62	0	0
IL-8	**403.83**	**4497.72**	**2501.13**	**1142.34**	**481.75**	**6356.2**	**3295.22**	**1104.18**	**573.39**	**11332.84**	**4000.53**	**1023.22**	**673.68**	**14104.83**	**3756.13**	**1135.05**
IL-9	20.26	60.02	45.63	34.8	43.74	104.69	91.52	47.26	85.87	138.9	123.32	84.9	111.39	150.2	132.51	87.79
IL-10	0	0	0	0	0	0	0	0	0	0	0	0	0	0.08	0	0

Continued

Chemokine	6 h				12 h				24 h				48 h			
	PBS	LPS	rBmpA	rBmpA+CuIIa	PBS	LPS	rBmpA	rBmpA+CuIIa	PBS	LPS	rBmpA	rBmpA+CuIIa	PBS	LPS	rBmpA	rBmpA+CuIIa
IL-12(P70)	0	0	0	0	0	0	0	0	0	0	0	0	0	0	0	0
IL-12(P40)	0	0	0	0	0	0	0	0	0	10.89	0	0	0	15.03	6.56	1.85
IL-13	0	0	0	0	0	0.08	0.04	0	0	0.15	0.08	0	0	0.15	0.08	0
IL-15	0	0	0	0	0	0	0	0	0	0	0	0	0	0	0	0
IL-16	0	1.6	1.03	0.74	0.14	4.02	2.96	0.74	0.45	8.67	4.81	2.69	2.15	13.17	7.9	6.37
IL-17	0	0.04	0	0	0	0.98	0.19	0	0	3.53	1.11	0.33	0.6	4.93	2.82	2.09
IL-18	0	0	0	0	0	0	0	0	0	0	0	0	0	0.12	0	0
IP-10/CXCL10	**8.96**	**323.67**	**207.32**	**46.74**	**44.89**	**927.1**	**680.19**	**53.14**	**82.83**	**1260.76**	**726.63**	**79.9**	**126.35**	**1467.13**	**835.63**	**69.42**
LIF	29.44	64.7	57.1	38.79	40.74	89.96	73.18	34.87	64.7	144.24	102.88	84.39	270.48	473.24	374.39	119.34
MCP-1/CCL2	**30.15**	**248.12**	**160.24**	**29.33**	**40.8**	**357.58**	**212.28**	**22.98**	**65.78**	**484.29**	**257.54**	**26.18**	**110.3**	**602.73**	**320.2**	**25.98**
MCP-3/CCL7	0	0	0	0	0	0	0	0	0	0.02	0	0	0	0.34	0.02	0
M-CSF	0	1.29	1.25	1.87	0.64	4.05	2.76	1.41	3.35	9.03	6.02	7.44	11.94	24.64	17.04	12.7
MIF	367.41	551.5	522.18	460.48	455.91	550.86	665.36	405.06	704.24	817.13	887.39	881.46	881.46	1118.13	1105.27	1263.34
MIG/CXCL9	0	0	0	0	0	0	0	0	0	1.44	0	0	0	2.84	0	0
MIP-1α/CCL3	0.55	7.75	2.73	2.27	1.05	14.71	4.68	3.69	3.68	62.79	17.21	16.67	10.74	161.64	43.32	38.53
MIP-1β	12.63	84.91	36.13	30.55	24.87	131.16	63.84	37.52	51.9	240.76	97.1	70.02	63.57	307.81	116.63	77.59
β-NGF	0	0	0	0	0	2.43	1.42	0	2.43	8.73	7.35	1.35	6.89	14.22	11.32	6.74
PDGF-BB	0	0	0	0	0	0	0	0	0	0	0.46	0	0	9.3	10.26	13.99
RANTES/CCL5	**32.05**	**96.68**	**80.97**	**65.97**	**109.62**	**396.18**	**282.99**	**92**	**450.35**	**1726.82**	**1131.34**	**365.36**	**1649.8**	**9075.17**	**6087.52**	**330.2**
SCF	0	1.74	1.09	0.43	0.2	3.87	1.95	0.65	0.87	7.02	3.45	2.6	2.6	10.56	5.97	5.76
SCGF-β	728.58	655.03	488.57	691.84	525.69	902.37	673.44	911.48	947.92	1310.18	1328.2	838.47	1346.22	1776.66	1436.2	966.12
SDF-1α	0	16.18	8.13	2.59	4.71	31.45	23.46	8.13	19.1	42.75	37.46	23.98	39.69	58.18	49.92	25.53
TNF-α	0.13	5.91	2.43	2.07	1.71	9.74	7.21	2.61	5.36	13.71	10.21	4.99	7.12	18.96	13.52	6.93

Continued

Chemokine	6 h				12 h				24 h				48 h			
	PBS	LPS	rBmpA	rBmpA+CuIIa	PBS	LPS	rBmpA	rBmpA+CuIIa	PBS	LPS	rBmpA	rBmpA+CuIIa	PBS	LPS	rBmpA	rBmpA+CuIIa
TNF-β	20.44	62.83	49.21	36.94	46.39	115.85	94.09	46.19	88.8	143.19	130.63	90.06	113.67	167.53	147.73	90.28
TRAIL	0	9.01	7.78	3.55	2.45	15.82	11.44	3.77	7.36	24.37	16.22	9.21	11.55	33.66	22.45	9.42
VEGF	0	0	0	0	0	0	0	0	73.95	118.11	84.56	199.38	1013.06	863.76	758.81	239.68

below the lower limit of detection. We used TBtools (Chen et al., 2020) to make a circular heatmap of the data of the 48 cytokines and the 24 cytokines with changes in expression, normalized the data by establishing logarithms, and performed a cluster analysis of the expressions, and the results are shown in Fig. 2. Through analysis, we found that the concentrations of the six cytokines (IL-6, IL-8, CCL2, CCL5, CXCL1, and CXCL10) increased significantly after LPS and rBmpA stimulation and decreased significantly after CuIIa treatment. These six factors are indicated in bold in Table 2. Furthermore, concentration of the six cytokines in the rBmpA group was at least two times greater than that in the negative control group and rBmpA plus CuIIa group. Therefore, we selected these six cytokines for further study.

3.3. Validation of cytokine mRNA expression in HMC3 cells by quantitative polymerase chain reaction

By analyzing the results of the cytokine array, we selected six factors for further study. We performed qPCR to verify if these six factors have the same changes in mRNA levels as in protein levels. The results of qPCR showed that, compared to the negative control group at the same time point, the relative expression of IL-6, IL-8, CCL2, CCL5, CXCL1, and CXCL10 mRNA increased significantly in both the LPS group and rBmpA group, and the difference was statistically significant. In contrast, the mRNA expression of these factors was significantly lower in the combination of rBmpA and CuIIa group compared with the rBmpA alone group, and the difference was statistically significant. In addition, with the prolongation of rBmpA action time, the mRNA expression of six factors showed a decreasing trend in rBmpA group (Fig. 3).

3.4. Validation of cytokine protein expression in HMC3 cells by ELISA

ELISA was used to confirm several chemokines that increased in the results of cytokine chip. Compared to the negative control group at the same time point, the concentration of IL-6, IL-8 and CXCL10 (pg/mL) increased significantly in the supernatants of both the LPS group and rBmpA experimental group, and the difference was statistically significant. In contrast, the concentration of these factors was significantly lower in the rBmpA plus CuIIa group compared with the rBmpA alone group, and the difference was statistically significant. Furthermore, with the prolongation of rBmpA action time, expression levels of IL-6, IL-8 and CXCL10 showed an increasing trend (Fig. 4).

4. Discussion

LNB is a neurological disease caused by *Bb* infection. Patients with LNB present with a variety of clinical manifestations in the central and peripheral nervous system, such as lymphocytic meningitis, cranial neuritis, and painful radiculitis (Koedel et al., 2015, Garcia-Monco and Benach, 2019). The presence of a large number of lipoproteins on the surface of *Bb* is associated with spirochete pathogenicity, and our previous study found that BmpA plays a key role in Lyme arthritis (Pal et al., 2008). In addition, BmpA can induce microglia in mice to produce a large number of cytokines associated with inflammation (Zhao et al., 2017b; 2017a). Therefore, we speculate that BmpA may be related to the pathogenesis of LNB, and microglia are closely related to LNB. Microglia are in fact vital participants in CNS homeostasis, and dysregulation of these sentinels can give rise to neurological disease (Nayak et al., 2014). Microglia detect extracellular changes in the brain and are rapidly activated in response to various noxious stimuli (Dello Russo et al., 2018, Morris et al., 2013). Microglia are resident macrophage-like immune cells in the CNS and play a vital role in both physiological and pathological conditions, including restoring the integrity of the CNS and promoting the progression of neurodegenerative disorders (Du et al., 2017). Inappropriate microglia activation has been implicated in several neurologic diseases (Colonna and Butovsky, 2017). Therefore, we speculated that microglia are involved in the pathogenesis of LNB and we chose HMC3 for the experiment.

In addition, it was found that some patients with LNB develop post-treatment Lyme disease syndrome after treatment with commonly used antibiotics, such as doxycycline and ceftriaxone (Kullberg et al., 2020), so it is important to explore new drugs for the treatment of LNB. Our previous study found that CuIIa has an inhibitory effect on BmpA-induced inflammation in human macrophages (Peng et al., 2020); therefore, in this study we investigate the effect of CuIIa on human microglia stimulated by the spirochete- dominant protein BmpA and what role it plays in microglia inflammation. We set up four groups, a normal cell group as a negative control group, LPS-stimulated group as a positive control group, and experimental groups including rBmpA-stimulated group and rBmpA plus CuIIa group. Cell seeding concentrations and rBmpA stimulation concentrations were determined by pre-experiments (Zhao et al., 2017b; 2017a, Li et al., 2021). The optimal concentration of CuIIa was determined by the CCK8 cell proliferation toxicity assay. We can see from Fig. 1 that when CuIIa concentration was 1 μM, CuIIa had a promoting effect on cell proliferation. This is an interesting phenomenon. We speculate that the low concentration of CuIIa may activate the pathway related to HMC3 cell proliferation, but this phenomenon and explanation need more experimental evidence, and we will carry out experiments to explore it in the future. In addition, the cell viability varied greatly at the three time points, so the concentration of 1 μM will not be used. At 100 and 200 μM concentrations of CuIIa, cell viability was low and decreased further with time, so these two concentrations are too toxic to use. Cell viability was relatively higher at 12.5 μM, 25 μM, and 50 μM of CuIIa and was stable between time points. Cell viability was highest at 50 μM, so we chose 50 μM as the experimental concentration. Since microglia are mainly found in the central nervous system, although we conducted an in vitro experiment, we simulated that CuIIa can directly act on microglia. At present, there are no studies to show whether CuIIa can cross the blood-brain barrier (BBB), and this question has a very high value and deserves our relevant research. In addition, if CuIIa cannot easily pass the BBB, we can take certain measures to enable it to pass the BBB, such as modifying the drug structure, of course, how to modify, still need to carry out a lot of experiments. What we want to say is that if we really need to do in vivo experiments, the question of whether or not CuIIa can cross the BBB must be considered.

LNB consists of neural inflammation, so we bring the supernatant of the cells stimulated by BmpA for cytokine array detection, and we choose Bio-Plex Pro Human Inflammation Assays (Bio-Rad, USA) that are related to human inflammation as the cytokine detection tool. Table 2 shows the array detection results. After analyzing the data, we found that 24 factors with significant changes were detected and the other 24 factors were not detected, probably because HMC3 was not secreted by them or their levels were below the lower limit of detection. We made two circular heat maps based on the expression of the 48 factors and the 24 factors detected with changes, and we normalized the data by constructing the logarithm and performing a cluster analysis based on the expression level, and the results are shown in Fig. 2. Finally, after analysis and screening, we found that six cytokines (CCL2, CCL5, CXCL1, CXCL10, IL-6, and IL-8) were significantly increased after LPS and rBmpA stimulation, while their levels were significantly decreased in the rBmpA plus CuIIa group. Therefore, we selected these six cytokines for further study.

Chemotaxis of leukocytes by chemotactic cytokines is an important initiating step in the inflammatory process and an important aspect of the innate immune function of the body to defend against and clear foreign bodies, such as invading pathogens (Zlotnik and Yoshie, 2000). Monocyte chemoattractant protein-1 (MCP-1/CCL2) is one of the key chemokines that regulate migration and infiltration of monocytes/macrophages (Deshmane et al., 2009). Both CCL2 and its receptor CCR2 have been demonstrated to be induced and involved in various diseases (Deshmane et al., 2009). RANTES, also known as CCL5, is a member of the CC subfamily of chemotactic cytokines and is released by

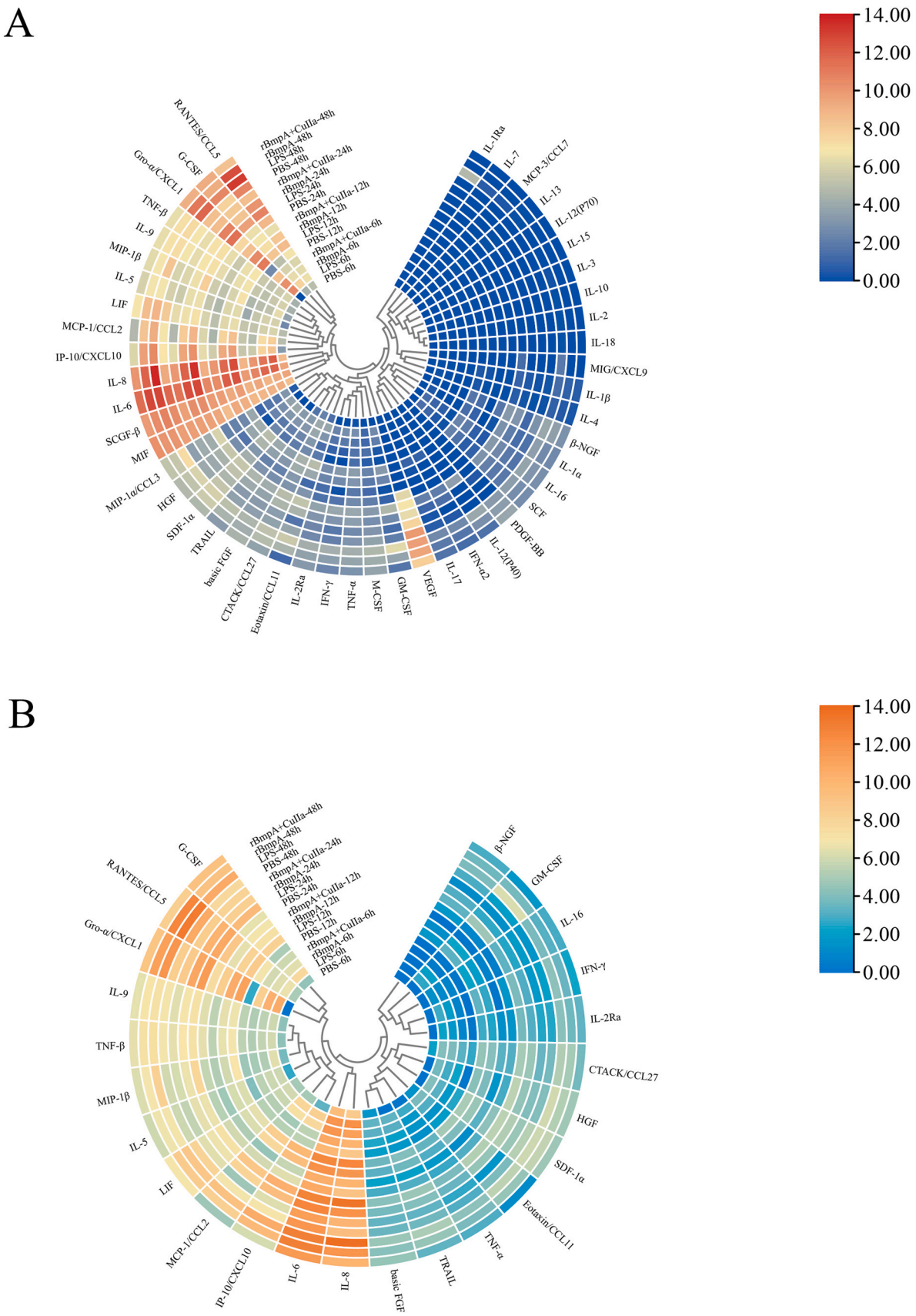

Fig. 2. The circular heatmap of expression. (A) Circular heatmap of 48 cytokines showing the hierarchical clustering of expression. High and low abundance of protein expression is shown in red and blue, respectively. (B) Circular heatmap of 24 increased cytokines. High and low abundance of protein expression is shown in yellow and blue, respectively.

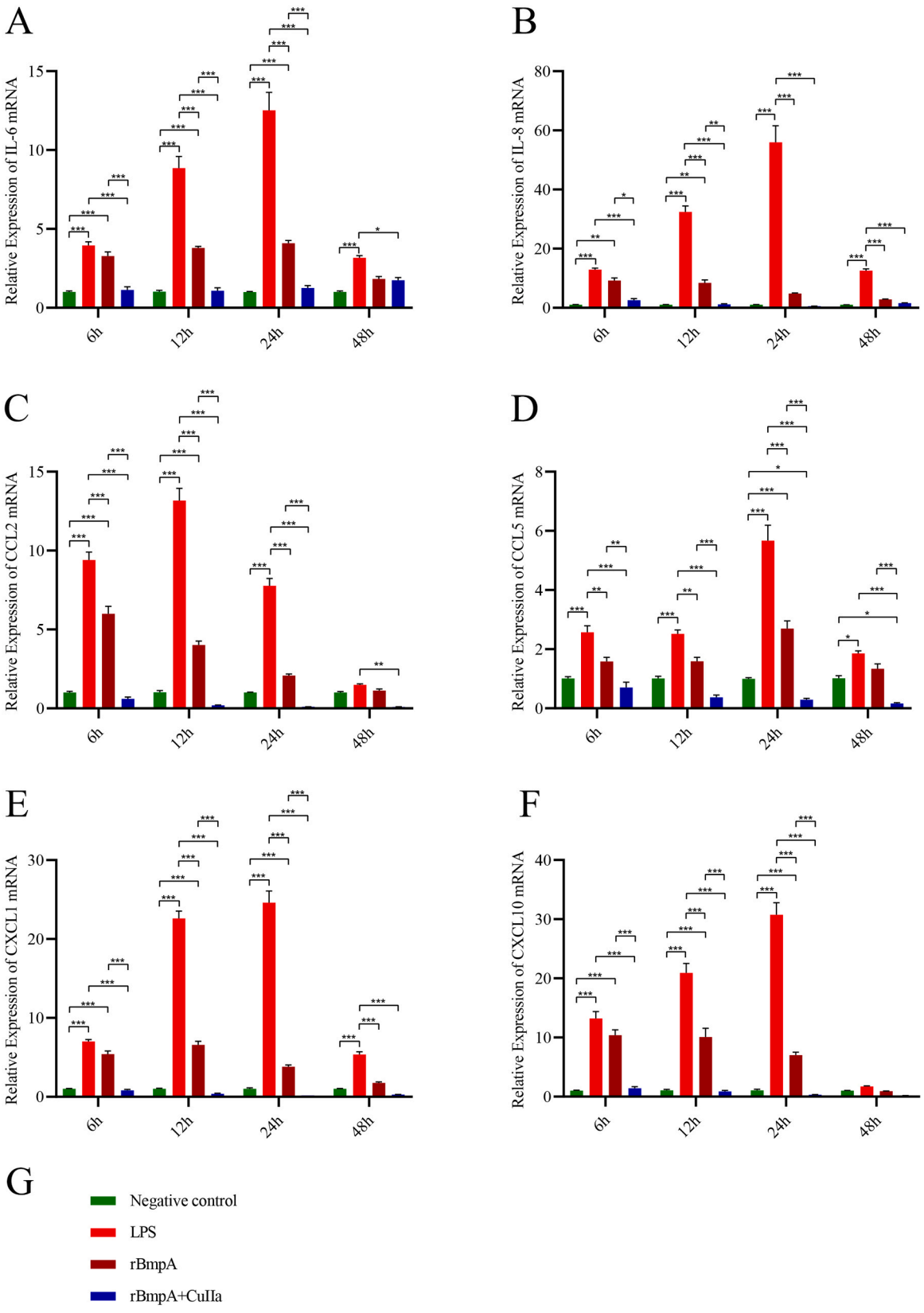

Fig. 3. Comparison of IL-6, IL-8, CCL2, CCL5, CXCL1, and CXCL10 mRNA relative expression in different groups at the same time. (A) IL-6. (B) IL-8. (C) CCL2. (D) CCL5. (E) CXCL1. (F) CXCL10. (G) Drawing statement. Compared to the negative control group at the same time point, the relative expression of IL-6, IL-8, CCL2, CCL5, CXCL1, and CXCL10 mRNA increased significantly in both the LPS group and rBmpA group, while the mRNA expression of these factors was significantly lower in the combination of rBmpA and CuIIa group compared with the rBmpA alone group. Two-way ANOVA and Tukey's multiple comparison test were used to evaluate the statistical significance between means and SEM of quadruplicate data sets, * $P < 0.05$, * * $P < 0.01$, * ** $P < 0.001$.

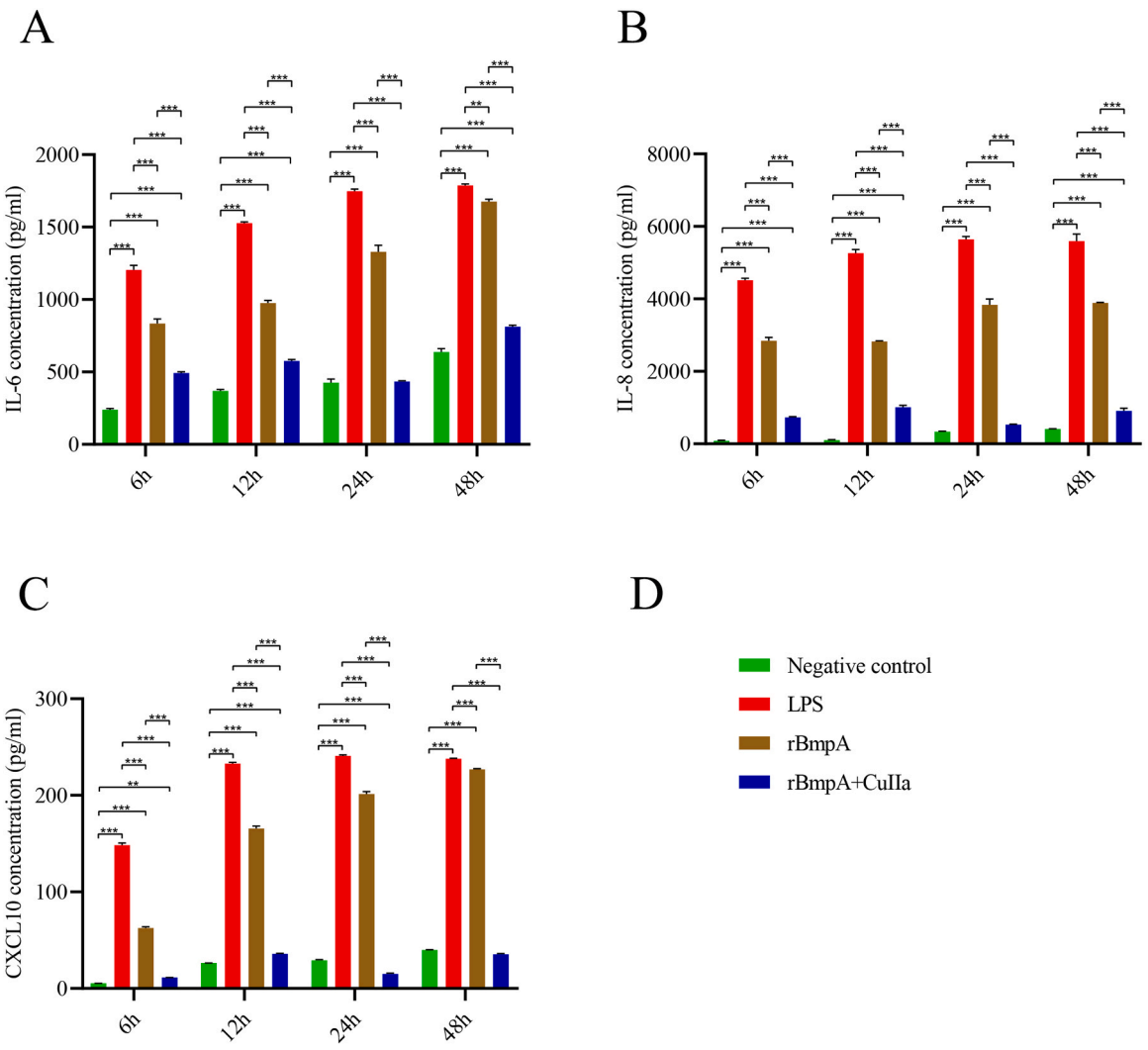

Fig. 4. Comparison of IL-6, IL-8, CXCL10 concentration of cells in different groups of the same time. (A) IL-6. (B) IL-8. (C) CXCL10. (D) Drawing statement. Compared with the negative control group, the expression levels of IL-6, IL-8 and CXCL10 were significantly increased in LPS group and rBmpA group, while significantly decreased in rBmpA plus CuIIa group. Two-way ANOVA and Tukey's multiple comparison test were used to evaluate the statistical significance between means and SEM of triplicate data sets, * $P < 0.05$, * * $P < 0.01$, * ** $P < 0.001$.

most tissues in response to stimulation by the inflammatory factors IL-1β or TNF-α. CCL5 is normally secreted mainly by CD8 + T cells, epithelial cells, fibroblasts, and platelets. CCL5 is chemotactic for a variety of leukocytes, such as monocytes, activated CD4 + T cells, and eosinophils. These properties give CCL5 an important role in immunomodulatory functions and in autoimmune disorders and inflammatory processes (Zlotnik and Yoshie, 2000). CXCL1 is a C-X-C chemokine family member containing a Glu-LeuArg (ELR) motif at its amino terminus. It is one of the major chemoattractants for neutrophils (De Filippo et al., 2008; 2013). CXCL1 expression is regulated mainly by nuclear factor-kappa B (NF-κB) and CCAAT-enhancer-binding proteins-β (C/EBPβ) (Acosta et al., 2008, Xu et al., 2014), which are transcription factors involved in expression of genes related to the inflammatory process (Pyle et al., 2017). Therefore, CXCL1 is a chemotactic cytokine produced during inflammation and is important for attracting polymorphonuclear cells toward the inflammatory site (Silva et al., 2017). CXCL10 also belongs to the ELR (-) CXC subfamily chemokine. CXCL10 exerts its function through binding to chemokine (C-X-C motif) receptor 3 (CXCR3), a seven trans-membrane receptor coupled to G proteins. CXCL10 and its receptor, CXCR3, appear to contribute to the pathogenesis of many autoimmune diseases, organ specific (such as type 1 diabetes, autoimmune thyroiditis and Graves' disease), or systemic (such as rheumatoid arthritis, psoriatic arthritis and systemic lupus erythematosus). A high level of CXCL10 in peripheral fluids is therefore a marker of host immune response, especially T helper (Th) 1 oriented T cells (Antonelli et al., 2014, Koper et al., 2018). IL-6 family cytokines have overlapping but also distinct biologic activities and are involved, among others, in the regulation of the hepatic acute phase reaction, in B-cell stimulation, in the regulation of the balance between regulatory and effector T cells, and in many neural functions (Rose-John, 2018). Interleukin-6 (IL-6), promptly and transiently produced in response to infections and tissue injuries, contributes to host defense through the stimulation of acute phase responses, hematopoiesis, and immune reactions. Although its expression is strictly controlled by transcriptional and post-transcriptional mechanisms, dysregulated continual synthesis of IL-6 has a pathological effect on chronic inflammation and autoimmunity (Tanaka et al., 2014). Interleukin-8 (IL-8) belongs to a family of small, structurally related cytokines similar to platelet factor 4. It is produced by phagocytes and mesenchymal cells exposed to inflammatory stimuli (e.g., interleukin-1 or tumor necrosis factor) and activates neutrophils to induce its chemotaxis, exocytosis, and the respiratory burst. IL-8 and the related cytokines are produced in several tissues upon infection, inflammation, ischemia, trauma etc., and are thought to be the main cause of local neutrophil accumulation (Baggiolini and Clark-Lewis,

1992).

Overall, these six cytokines are closely associated with the development of inflammation and they may be related to the pathogenesis of LNB. We selected these six factors to validate their expression in the mRNA level and observe whether the mRNA results were consistent with the trend in protein level changes. Fig. 3 represents the comparison between different groups at the same time point for the six cytokines. The results showed that mRNA expression of the six cytokines increased after rBmpA stimulation of HMC3 compared to the negative control group, while in the rBmpA plus CuIIa group, the mRNA expression of the six chemokines was decreased. Thus, our results demonstrated again at the mRNA level that rBmpA can induce the production of cytokines by HMC3, while CuIIa can inhibit their expression. In addition, from the figure we can see that in the negative control group, the mRNA levels of the six cytokines at four time points were not statistically different, in accordance with the experimental requirements. However, in the LPS-stimulated group, the mRNA expression of the six cytokines was high at 6, 12, and 24 h and decreased at 48 h; it is possible that the cell stress response decreased with time. Similarly, we observed that the mRNA levels of the six cytokines dropped at 48 h in the rBmpA stimulated group, probably also for this reason. In addition to qPCR, we selected 3 cytokines for ELISA to further verify the results of cytokine chip, and the ELISA results were consistent with mRNA expression results (Fig. 4). In addition, from the Fig. 4, IL-6 and CXCL10 gradually increased in untreated cells. Studies have shown that, on the one hand, IL-6 and CXCL10 are closely related to the inflammatory response of cells (Koper et al., 2018, Tanaka et al., 2014), and some stress responses of cells may gradually increase during cell culture, resulting in increased secretion of IL-6 and CXCL10. On the other hand, the cells in the untreated group continued to proliferate, which may also explain the gradually increase in IL-6 and CXCL10. Studies have shown that LPS activates the TLR2/4 signaling pathway of microglia, and Cucurbitacins pretreatment significantly reduces the pro-inflammatory cytokines (TNF-α, IL-1β, and IL-6) of LPS-stimulated microglia, as well as the expression of iNOS and COX-2 (Peng et al., 2020, Zhao et al., 2019). In addition, Cucurbitacins inhibited the activation of JNK and p38 MAPKs in TLR 2/4-stimulated microglia and attenuated the activation of JAK-STAT and NF-κB (Boykin et al., 2011, Park et al., 2015) As for the activation cascade of rBmpA on microglia, we are also looking forward to follow-up studies.

Our study demonstrated at the protein level and mRNA level that rBmpA can induce a high production of cytokines in human microglia HMC3, leading to the occurrence of inflammation, which may be one of the mechanisms of LNB pathogenesis. In addition, in the present study we demonstrated for the first time the inhibitory effect of CuIIa on rBmpA-induced inflammation in HMC3 cells. Our results may support the potential of CuIIa for the treatment of LNB. Besides, the mechanism of rBmpA-induced HMC3 production of cytokines and the anti-inflammatory mechanism of CuIIa are still unclear, and we will address these questions in depth in future research. We will also continue to advance the study of LNB pathogenesis in experiments in vivo or organoid models.

5. Conclusion

The surface protein BmpA of *Bb* can stimulate the human microglia cell line HMC3 to produce large amounts of cytokines, leading to the occurrence of inflammation, so BmpA may be closely related to the development of LNB. CuIIa can inhibit BmpA-induced cytokine production by HMC3, which may have potential therapeutic effects on LNB. These findings may provide insights to prevent and treat LNB.

Funding

This work was supported by grants from the National Natural Science Foundation of China (No. 32060180, 82160304, and 81860644), Yunnan Province Department of Science and Technology-Kunming Medical University Joint Fund Projects [No. 2019FE001 (−002) and 2017FE467 (-001)].

CRediT authorship contribution statement

Shiyuan Wen: Conceptualization, Formal analysis. Meixiao Liu: Conceptualization, Formal analysis. **Yuxin Fan:** Conceptualization, Formal analysis. Jingjing Chen: Conceptualization, Formal analysis. **Zhenhua Ji:** Conceptualization, Formal analysis. **Yan Dong:** Conceptualization, Formal analysis. **Yu Zhang:** Methodology. **Wenjing Cao:** Methodology. **Peng Yue:** Methodology. **Jing Kong:** Methodology. **Aihua Liu:** Supervision. **Fukai Bao:** Supervision. **Guozhong Zhou:** Visualization. **Bingxue Li:** Visualization. **Xin Xu:** Writing – original draft. All authors have read and agreed to the published version of the manuscript.

Declaration of Competing Interest

The funders had no role in the design of the study; in the collection, analyses, or interpretation of data; in the writing of the manuscript; or in the decision to publish the results.

References

Acosta, J.C., O'loghlen, A., Banito, A., Guijarro, M.V., Augert, A., Raguz, S., Fumagalli, M., Da Costa, M., Brown, C., Popov, N., Takatsu, Y., Melamed, J., D'adda Di Fagagna, F., Bernard, D., Hernando, E., Gil, J., 2008. Chemokine signaling via the CXCR2 receptor reinforces senescence. Cell 133, 1006–1018. https://doi.org/10.1016/j.cell.2008.03.038.

Aloisi, F., 2001. Immune function of microglia. Glia 36, 165–179. https://doi.org/10.1002/glia.1106.

Angel-Ambrocio, A.H., Bautista-Carbajal, P., García-León, M.L., Gomora-Herrera, M.J., Pedernera-Astegiano, E.A., Wong-Chew, R.M., 2020. Microglia HMC3 cells are highly susceptible to rhinovirus infection. Virus Res 288, 198110. https://doi.org/10.1016/j.virusres.2020.198110.

Antonelli, A., Ferrari, S.M., Giuggioli, D., Ferrannini, E., Ferri, C., Fallahi, P., 2014. Chemokine (C-X-C motif) ligand (CXCL)10 in autoimmune diseases. Autoimmun. Rev. 13, 272–280. https://doi.org/10.1016/j.autrev.2013.10.010.

Baggiolini, M., Clark-Lewis, I., 1992. Interleukin-8, a chemotactic and inflammatory cytokine. FEBS Lett. 307, 97–101. https://doi.org/10.1016/0014-5793(92)80909-z.

Boykin, C., Zhang, G., Chen, Y.H., Zhang, R.W., Fan, X.E., Yang, W.M., Lu, Q., 2011. Cucurbitacin IIa: a novel class of anti-cancer drug inducing non-reversible actin aggregation and inhibiting survivin independent of jak2/stat3 phosphorylation. Br. J. Cancer 104, 781–789. https://doi.org/10.1038/bjc.2011.10.

Cai, Y., Fang, X., He, C., Li, P., Xiao, F., Wang, Y., Chen, M., 2015. Cucurbitacins: a systematic review of the phytochemistry and anticancer activity. Am. J. Chin. Med 43, 1331–1350. https://doi.org/10.1142/s0192415x15500755.

Cardoso, L.S., Araujo, M.I., Góes, A.M., Pacífico, L.G., Oliveira, R.R., Oliveira, S.C., 2007. Polymyxin b as inhibitor of LPS contamination of Schistosoma mansoni recombinant proteins in human cytokine analysis. Micro Cell Fact. 6 (1) https://doi.org/10.1186/1475-2859-6-1.

Chen, C., Chen, H., Zhang, Y., Thomas, H.R., Frank, M.H., He, Y., Xia, R., 2020. Tbtools: an integrative toolkit developed for interactive analyses of big biological data. Mol. Plant 13, 1194–1202. https://doi.org/10.1016/j.molp.2020.06.009.

Colonna, M., Butovsky, O., 2017. Microglia function in the central nervous system during health and neurodegeneration. Annu Rev. Immunol. 35, 441–468. https://doi.org/10.1146/annurev-immunol-051116-052358.

Cooper, J.F., Hochstein, H.D., Seligmann Jr., E.B., 1972. The limulus test for endotoxin (pyrogen) in radiopharmaceuticals and biologicals. Bull. Parent. Drug Assoc. 26, 153–162.

De Filippo, K., Henderson, R.B., Laschinger, M., Hogg, N., 2008. Neutrophil chemokines KC and macrophage-inflammatory protein-2 are newly synthesized by tissue macrophages using distinct TLR signaling pathways. J. Immunol. 180, 4308–4315. https://doi.org/10.4049/jimmunol.180.6.4308.

De Filippo, K., Dudeck, A., Hasenberg, M., Nye, E., Van Rooijen, N., Hartmann, K., Gunzer, M., Roers, A., Hogg, N., 2013. Mast cell and macrophage chemokines CXCL1/CXCL2 control the early stage of neutrophil recruitment during tissue inflammation. Blood 121, 4930–4937. https://doi.org/10.1182/blood-2013-02-486217.

Delgado-Tiburcio, E.E., Cadena-Iñiguez, J., Santiago-Osorio, E., Ruiz-Posadas, L.D.M., Castillo-Juárez, I., Aguiñiga-Sánchez, I., Soto-Hernández, M., 2022. Pharmacokinetics and biological activity of cucurbitacins. Pharmaceuticals 15. https://doi.org/10.3390/ph15111325.

Dello Russo, C., Cappoli, N., Coletta, I., Mezzogori, D., Paciello, F., Pozzoli, G., Navarra, P., Battaglia, A., 2018. The human microglial HMC3 cell line: where do we stand? A systematic literature review. J. Neuroinflamm. 15, 259 https://doi.org/10.1186/s12974-018-1288-0.

Deshmane, S.L., Kremlev, S., Amini, S., Sawaya, B.E., 2009. Monocyte chemoattractant protein-1 (MCP-1): an overview. J. Interferon Cytokine Res 29, 313–326. https://doi.org/10.1089/jir.2008.0027.

Du, L., Zhang, Y., Chen, Y., Zhu, J., Yang, Y., Zhang, H.L., 2017. Role of microglia in neurological disorders and their potentials as a therapeutic target. Mol. Neurobiol. 54, 7567–7584. https://doi.org/10.1007/s12035-016-0245-0.

Garcia-Monco, J.C., Benach, J.L., 2019. Lyme neuroborreliosis: clinical outcomes, controversy, pathogenesis, and polymicrobial infections. Ann. Neurol. 85, 21–31. https://doi.org/10.1002/ana.25389.

Halperin, J.J., 2014. Nervous system lyme disease. Handb. Clin. Neurol. 121, 1473–1483. https://doi.org/10.1016/b978-0-7020-4088-7.00099-7.

Hankittichai, P., Lou, H.J., Wikan, N., Smith, D.R., Potikanond, S., Nimlamool, W., 2020. Oxyresveratrol inhibits IL-1β-induced inflammation via suppressing AKT and ERK1/2 activation in human microglia, HMC3. Int J. Mol. Sci. 21 https://doi.org/10.3390/ijms21176054.

Isogai, E., Isogai, H., Kimura, K., Hayashi, S., Kubota, T., Nishikawa, T., Nakane, A., Fujii, N., 1996. Cytokines in the serum and brain in mice infected with distinct species of Lyme disease borrelia. Micro Pathog. 21, 413–419. https://doi.org/10.1006/mpat.1996.0072.

Koedel, U., Pfister, H.W., 2017. Lyme neuroborreliosis. Curr. Opin. Infect. Dis. 30, 101–107. https://doi.org/10.1097/qco.0000000000000332.

Koedel, U., Fingerle, V., Pfister, H.W., 2015. Lyme neuroborreliosis-epidemiology, diagnosis and management. Nat. Rev. Neurol. 11, 446–456. https://doi.org/10.1038/nrneurol.2015.121.

Koper, O.M., Kamińska, J., Sawicki, K., Kemona, H., 2018. CXCL9, CXCL10, CXCL11, and their receptor (CXCR3) in neuroinflammation and neurodegeneration. Adv. Clin. Exp. Med 27, 849–856. https://doi.org/10.17219/acem/68846.

Kullberg, B.J., Vrijmoeth, H.D., Van De Schoor, F., Hovius, J.W., 2020. Lyme borreliosis: Diagnosis and management. Bmj 369, m1041. https://doi.org/10.1136/bmj.m1041.

Li, L., Luo, L., Chen, T., Cao, W., Xu, X., Zhang, Y., Yue, P., Fan, Y., Chen, J., Liu, M., Ma, M., Tao, L., Peng, Y., Dong, Y., Li, B., Luo, S., Kong, J., Zhou, G., Wen, S., Liu, A., Bao, F., 2021. Proteomic analysis of rhesus macaque brain explants treated with *Borrelia burgdorferi* identifies host GAP-43 as a potential factor associated with Lyme neuroborreliosis. Front Cell Infect. Microbiol 11, 647662. https://doi.org/10.3389/fcimb.2021.647662.

Marques, A.R., 2015. Lyme neuroborreliosis. Contin. (Minne Minn. 21, 1729–1744. https://doi.org/10.1212/con.0000000000000252.

Morris, G.P., Clark, I.A., Zinn, R., Vissel, B., 2013. Microglia: A new frontier for synaptic plasticity, learning and memory, and neurodegenerative disease research. Neurobiol. Learn Mem. 105, 40–53. https://doi.org/10.1016/j.nlm.2013.07.002.

Nayak, D., Roth, T.L., Mcgavern, D.B., 2014. Microglia development and function. Annu Rev. Immunol. 32, 367–402. https://doi.org/10.1146/annurev-immunol-032713-120240.

Pachner, A.R., Steiner, I., 2007. Lyme neuroborreliosis: infection, immunity, and inflammation. Lancet Neurol. 6, 544–552. https://doi.org/10.1016/s1474-4422(07)70128-x.

Pachner, A.R., Dail, D., Narayan, K., Dutta, K., Cadavid, D., 2002. Increased expression of b-lymphocyte chemoattractant, but not pro-inflammatory cytokines, in muscle tissue in rhesus chronic Lyme borreliosis. Cytokine 19, 297–307. https://doi.org/10.1006/cyto.2002.1973.

Pal, U., Wang, P., Bao, F., Yang, X., Samanta, S., Schoen, R., Wormser, G.P., Schwartz, I., Fikrig, E., 2008. *Borrelia burgdorferi* basic membrane proteins A and B participate in the genesis of Lyme arthritis. J. Exp. Med 205, 133–141. https://doi.org/10.1084/jem.20070962.

Park, S.Y., Kim, Y.H., Park, G., 2015. Cucurbitacins attenuate microglial activation and protect from neuroinflammatory injury through Nrf2/ARE activation and STAT/NF-κB inhibition. Neurosci. Lett. 609, 129–136. https://doi.org/10.1016/j.neulet.2015.10.022.

Peng, Y., Chen, T., Luo, L., Li, L., Cao, W., Xu, X., Zhang, Y., Yue, P., Dai, X., Ji, Z., Jian, M., Bai, R., Ding, Z., Wang, F., Wen, S., Zhou, G., Kong, J., Luo, S., Liu, A., Bao, F., 2020. Isoforskolin and cucurbitacin IIa promote the expression of anti-inflammatory regulatory factor sigirr in human macrophages stimulated with *Borrelia burgdorferi* basic membrane protein A. Int Immunopharmacol. 88, 106914 https://doi.org/10.1016/j.intimp.2020.106914.

Pyle, C.J., Akhter, S., Bao, S., Dodd, C.E., Schlesinger, L.S., Knoell, D.L., 2017. Zinc modulates endotoxin-induced human macrophage inflammation through ZIP8 induction and C/EBPβ inhibition. PLoS One 12, e0169531. https://doi.org/10.1371/journal.pone.0169531.

Recio, M.C., Prieto, M., Bonucelli, M., Orsi, C., Máñez, S., Giner, R.M., Cerdá-Nicolás, M., Ríos, J.L., 2004. Anti-inflammatory activity of two cucurbitacins isolated from *Cayaponia tayuya* roots. Planta Med 70, 414–420. https://doi.org/10.1055/s-2004-818968.

Rose-John, S., 2018. Interleukin-6 family cytokines. Cold Spring Harb. Perspect. Biol. 10 https://doi.org/10.1101/cshperspect.a028415.

Silva, R.L., Lopes, A.H., Guimarães, R.M., Cunha, T.M., 2017. CXCL1/CXCR2 signaling in pathological pain: role in peripheral and central sensitization. Neurobiol. Dis. 105, 109–116. https://doi.org/10.1016/j.nbd.2017.06.001.

Silvestre, G.F.G., De Lucena, R.P., Da Silva Alves, H., 2022. Cucurbitacins and the immune system: Update in research on anti- inflammatory, antioxidant, and immunomodulatory mechanisms. Curr. Med Chem. 29, 3774–3789. https://doi.org/10.2174/0929867329666220107153253.

Tanaka, T., Narazaki, M., Kishimoto, T., 2014. IL-6 in inflammation, immunity, and disease. Cold Spring Harb. Perspect. Biol. 6, a016295. https://doi.org/10.1101/cshperspect.a016295.

Tsuzuki, H., Tani, T., Ueyama, H., Kodama, M., 2001. Lipopolysaccharide: Neutralization by polymyxin b shuts down the signaling pathway of nuclear factor kappab in peripheral blood mononuclear cells, even during activation. J. Surg. Res 100, 127–134. https://doi.org/10.1006/jsre.2001.6227.

Varela, C., Melim, C., Neves, B.G., Sharifi-Rad, J., Calina, D., Mamurova, A., Cabral, C., 2022. Cucurbitacins as potential anticancer agents: New insights on molecular mechanisms. J. Transl. Med 20, 630. https://doi.org/10.1186/s12967-022-03828-3.

Wang, X., Tanaka, M., Peixoto, H.S., Wink, M., 2017. Cucurbitacins: elucidation of their interactions with the cytoskeleton. PeerJ 5, e3357. https://doi.org/10.7717/peerj.3357.

Xu, J., Zhu, M.D., Zhang, X., Tian, H., Zhang, J.H., Wu, X.B., Gao, Y.J., 2014. NFκB-mediated CXCL1 production in spinal cord astrocytes contributes to the maintenance of bone cancer pain in mice. J. Neuroinflamm. 11, 38 https://doi.org/10.1186/1742-2094-11-38.

Yang, X., Izadi, H., Coleman, A.S., Wang, P., Ma, Y., Fikrig, E., Anguita, J., Pal, U., 2008. *Borrelia burgdorferi* lipoprotein BmpA activates pro-inflammatory responses in human synovial cells through a protein moiety. Microbes Infect. 10, 1300–1308. https://doi.org/10.1016/j.micinf.2008.07.029.

Zeng, Y., Wang, J., Huang, Q., Ren, Y., Li, T., Zhang, X., Yao, R., Sun, J., 2021. Cucurbitacin IIa: a review of phytochemistry and pharmacology. Phytother. Res. https://doi.org/10.1002/ptr.7077.

Zhao, H., Liu, A., Cui, Y., Liang, Z., Li, B., Bao, F., 2017a. *Borrelia burgdorferi* basic membrane protein A could induce chemokine production in murine microglia cell line BV2. Micro Pathog. 111, 174–181. https://doi.org/10.1016/j.micpath.2017.08.036.

Zhao, H., Liu, A., Shen, L., Xu, C., Zhu, Z., Yang, J., Han, X., Bao, F., Yang, W., 2017b. Isoforskolin downregulates proinflammatory responses induced by *Borrelia burgdorferi* basic membrane protein A. Exp. Ther. Med 14, 5974–5980. https://doi.org/10.3892/etm.2017.5300.

Zhao, H., Dai, X., Han, X., Liu, A., Bao, F., Bai, R., Ji, Z., Jian, M., Ding, Z., Abi, M.E., Chen, T., Luo, L., Ma, M., Tao, L., 2019. *Borrelia burgdorferi* basic membrane protein A initiates proinflammatory chemokine storm in THP 1-derived macrophages via the receptors TLR1 and TLR2. Biomed. Pharm. 115, 108874 https://doi.org/10.1016/j.biopha.2019.108874.

Zhou, S.M., Guan, S.Y., Yang, L., Yang, L.K., Wang, L., Nie, H.F., Li, X., Zhao, M.G., Yang, Q., Wu, H., 2017. Cucurbitacin IIa exerts antidepressant-like effects on mice exposed to chronic unpredictable mild stress. Neuroreport 28, 259–267. https://doi.org/10.1097/wnr.0000000000000747.

Zlotnik, A., Yoshie, O., 2000. Chemokines: a new classification system and their role in immunity. Immunity 12, 121–127. https://doi.org/10.1016/s1074-7613(00)80165-x.